PET Imaging of System x_C^- in Immune Cells for Assessment of Disease Activity in Mice and Patients with Inflammatory Bowel Disease

Minjung Seo*[1], Yeji Kim*[2], Byong Duk Ye*[3], Sang Hyoung Park[3], Seog-Young Kim[2], Jin Hwa Jung[2], Sung Wook Hwang[3], Sun Young Chae[4], Dong Yun Lee[4], Sang Ju Lee[4], Seung Jun Oh[4], Jihun Kim[5], Ji Young Kim[6], Sae Jung Na[7], Misung Kim[8], Sang-Yeob Kim[2], Norman Koglin[9], Andrew W. Stephens[9], Mi-Na Kweon[2], and Dae Hyuk Moon[4]

[1]*Department of Nuclear Medicine, Ulsan University Hospital, University of Ulsan College of Medicine, Ulsan, Republic of Korea;* [2]*Department of Convergence Medicine, Asan Medical Center, University of Ulsan College of Medicine, Seoul, Republic of Korea;* [3]*Department of Gastroenterology, Asan Medical Center, University of Ulsan College of Medicine, Seoul, Republic of Korea;* [4]*Department of Nuclear Medicine, Asan Medical Center, University of Ulsan College of Medicine, Seoul, Republic of Korea;* [5]*Department of Pathology, Asan Medical Center, University of Ulsan College of Medicine, Seoul, Republic of Korea;* [6]*Department of Nuclear Medicine, Hanyang University Medical Center, Hanyang University College of Medicine, Seoul, Republic of Korea;* [7]*Department of Radiology, Uijeongbu St. Mary's Hospital, College of Medicine, Catholic University of Korea, Seoul, Republic of Korea;* [8]*Department of Pathology, Ulsan University Hospital, Ulsan, Republic of Korea; and* [9]*Life Molecular Imaging GmbH, Berlin, Germany*

We aimed to explore whether the imaging of antiporter system x_C^- of immune cells with (4*S*)-4-(3-^{18}F-fluoropropyl)-L-glutamate (^{18}F-FSPG) PET can assess inflammatory bowel disease (IBD) activity in murine models and patients (NCT03546868). **Methods:** ^{18}F-FSPG PET imaging was performed to assess IBD activity in mice with dextran sulfate sodium-induced and adoptive T-cell transfer–induced IBD and a cohort of 20 patients at a tertiary care center in South Korea. Immunohistochemical analysis of system x_C^- and cell surface markers was also studied. **Results:** Mice with experimental IBD showed increased intestinal ^{18}F-FSPG uptake and xCT expression in cells positive (+) for CD11c, F4/80, and CD3 in the lamina propria, increases positively associated with clinical and pathologic disease activity. ^{18}F-FSPG PET studies in patients, most of whom were clinically in remission or had mildly active IBD, showed that PET imaging was sufficiently accurate in diagnosing endoscopically active IBD and remission in patients and bowel segments. ^{18}F-FSPG PET correctly identified all 9 patients with superficial or deep ulcers. Quantitative intestinal ^{18}F-FSPG uptake was strongly associated with endoscopic indices of IBD activity. The number of $CD68^+xCT^+$ and $CD3^+xCT^+$ cells in 22 bowel segments from patients with ulcerative colitis and the number of $CD68^+xCT^+$ cells in 7 bowel segments from patients with Crohn disease showed a significant positive association with endoscopic indices of IBD activity. **Conclusion:** The assessment of system x_C^- in immune cells may provide diagnostic information on the immune responses responsible for chronic active inflammation in IBD. ^{18}F-FSPG PET imaging of system x_C^- activity may noninvasively assess the IBD activity.

Key Words: system x_C^-; immune cells; PET; inflammatory bowel disease

J Nucl Med 2022; 63:1586–1591
DOI: 10.2967/jnumed.121.263289

Received Oct. 6, 2021; revision accepted Jan. 18, 2022.
For correspondence or reprints, contact Dae Hyuk Moon (dhmoon@amc.seoul.kr) or Mi-Na Kweon (mnkweon@amc.seoul.kr).
*Contributed equally to this work.
Published online Jan. 27, 2022.

Inflammatory bowel disease (IBD) consists of 2 types of chronic incurable intestinal disorders, ulcerative colitis (UC) and Crohn disease (CD). Tight monitoring of disease activity is essential throughout the course of the disease to guide therapeutic decisions and assess response to therapy and relapse (*1,2*). Although endoscopic mucosal healing is a long-term goal of therapy, endoscopic evaluation may not always be feasible because of lack of immediate availability, cost, need for bowel preparation, relatively poor patient acceptance, and complications. Less invasive markers of disease activity are therefore needed.

Key immune processes involved in the pathogenesis of IBD include cytokine production by activated dendritic cells and macrophages, and the development of effector T lymphocyte subsets (*3*). Targeting dysfunctional immune cells and their products has led to the development of new therapies that have benefited patients (*3*). Similarly, a noninvasive method that targets dysfunctional immune cells, distinguishing between active cell subsets and quiescent cell populations, may allow specific assessment of disease activity, rather than relying on nonspecific indicators of disease activity (*4*).

System x_C^- plays an important role in the regulation of the innate and adaptive immune systems (*5*) and is upregulated in activated macrophages (*6,7*). On antigen stimulation, proliferating T cells require sufficient glutathione levels to ensure proper reactive oxygen species balance, resulting in the induction of high levels of xCT for cystine uptake (*8,9*). An *ex vivo* study on patients with IBD has shown that intestinal lamina propria macrophages expressed xCT, which resulted in high glutathione levels and full T-cell receptor reactivity (*10*). All these results suggest that system x_C^- could be a specific indicator of disease activity in IBD. Research designed to characterize the functional relevance of system x_C^- in disease states with oxidative stress and inflammation might pave the way for diagnosing and treating IBD (*5*).

(4*S*)-4-(3-^{18}F-fluoropropyl)-L-glutamate (^{18}F-FSPG) is a ^{18}F-labeled L-glutamate derivative that is specifically taken up by system x_C^- (*11*). An exploratory clinical study has shown that ^{18}F-FSPG PET can detect inflammation of the lungs and sarcoidosis (*12*). The low

background uptake of ^{18}F-FSPG would be especially advantageous in detecting inflammatory lesions in the intestine (*12,13*), an organ in which the use of conventional ^{18}F-FDG imaging may be limited because of physiologic uptake. ^{18}F-FDG PET may also be limited in differentiating mildly active IBD from endoscopic remission (*14,15*), showing an adequate accuracy only for detecting moderate-to-severe endoscopic disease (*16,17*). The objective of this study was to evaluate whether the *in vivo* assessment of system x_C^- in immune cells provides information on the dysregulated immune responses responsible for chronic active inflammation in IBD, thereby assessing the disease activity. We first conducted animal experiments to investigate whether ^{18}F-FSPG would have increased accumulation associated with xCT expression in immune cells. Second, we aimed to explore the diagnostic validity of ^{18}F-FSPG PET/CT in patients. Finally, we assessed the association of ^{18}F-FSPG uptake and xCT expression in immune cells with endoscopic markers.

MATERIALS AND METHODS

Experimental IBD Models, ^{18}F-FSPG PET Imaging, and *Ex Vivo* Analysis

The research protocol was approved by the Institutional Animal Care and Use Committee (registration numbers 2016-12-153 and 2017-12-017). All animal experiments conformed to the institutional guidelines. Experimental details are reported in accordance with the ARRIVE guidelines, version 2.0 (Animal Research: Reporting of In Vivo Experiments). Dextran sulfate sodium (DSS)–induced and adoptive T-cell transfer–induced IBD models were evaluated. Details of clinical disease activity, *ex vivo* analysis, and immunohistochemical staining for expression of xCT and cell surface markers are provided in the supplemental methods (supplemental materials are available at http://jnm.snmjournals.org).

Clinical Study Design and Patients

This was a prospective, nonrandomized, single-center cohort study. The study protocol, provided in the supplemental materials, was approved by the Ministry of Food and Drug Safety of the Republic of Korea and the institutional review board of Asan Medical Center (approval 2018-0262). This trial was conducted in accordance with the Declaration of Helsinki and institutional guidelines. All patients provided written informed consent before participation. The primary objective was to explore the validity of ^{18}F-FSPG PET/CT for the diagnosis of patients with active IBD. The secondary objectives were to explore the validity of ^{18}F-FSPG PET/CT for detecting bowel segments with active IBD; to assess the correlation of ^{18}F-FSPG activity with clinical, endoscopic, and biologic markers of disease activity; to assess the interreader variability of visual ^{18}F-FSPG PET/CT interpretation, and to evaluate the safety of ^{18}F-FSPG PET/CT. Intended enrollment included 10 patients with UC and 10 with CD, numbers regarded as sufficient to obtain PET/CT imaging information while avoiding unnecessary exposure to ionizing radiation. The trial was registered at http://clinicaltrials.gov as NCT03546868.

Patients eligible for inclusion were consecutive adults aged between 19 and 79 y who had UC or CD, as diagnosed clinically, endoscopically, and histologically. The complete inclusion and exclusion criteria are listed in the supplemental methods. All cases were identified on the basis of presenting symptoms, as evaluated by 3 of the authors at the Department of Gastroenterology.

^{18}F-FSPG PET/CT Imaging of Patients

Patients were asked to fast for at least 4 h before being administered ^{18}F-FSPG (8 h if they were on a high-protein diet). A dose of 200 ± 20 MBq of ^{18}F-FSPG was administered as a slow intravenous bolus injection for up to 60 s. Sixty minutes later, PET/CT was performed from the abdomen to the pelvis, with an acquisition time of 3 min per bed position, using a PET/CT scanner (Discovery PET/CT 690; GE Healthcare). The total radiation exposure from the CT examination did not exceed 1 mSv. Hyoscine butylbromide was administered intravenously before or during the PET/CT to reduce peristaltic movement. The safety assessment of ^{18}F-FSPG is provided in the supplemental methods.

Images were interpreted independently by 2 board-certified nuclear medicine physicians who were masked to clinical and endoscopic data. ^{18}F-FSPG intensity moderately higher than in the liver was considered positive for active disease. The SUV_{max} of each bowel segment was also determined, with the summed SUV_{max} being the sum of all segments. Disagreements between the 2 physicians were resolved by consensus. Details are provided in the supplemental methods (*12,13*).

Assessment of Disease Activity

Endoscopic assessment was considered a valid reference standard for disease activity and extent. Sigmoidoscopy or colonoscopy was performed by an experienced gastroenterologist masked to ^{18}F-FSPG PET/CT results. The severity and extent of inflammatory lesions were evaluated using the UC Endoscopic Index of Severity (UCEIS) in UC patients and the CD Endoscopic Index of Severity (CDEIS) in CD patients (*18*). Segmental scores were determined in 5 bowel segments per patient using the UCEIS or CDEIS. For segmental CDEIS, the score for ulcerated or nonulcerated stenosis was imputed to the affected segment. Endoscopic evidence of active UC was defined as a UCEIS score of at least 2, whereas endoscopic evidence of active CD was defined as a CDEIS score of at least 3. Bowel segments with a superficial or deep ulcer were considered severe disease. Clinical and pathologic assessment are summarized as the supplemental methods (*18*).

Immunohistochemical Staining of Human xCT, GLUT1, and Cell Surface Markers

The immunohistochemistry study was approved by the institutional review board of Asan Medical Center (approval 2019-0260). Written informed consent was obtained again from all participants. The details are summarized in the supplemental methods (*19*) and Supplemental Table 1.

Statistical Analysis

The sensitivity of ^{18}F-FSPG PET/CT for the diagnosis of endoscopic evidence of active disease was calculated as the probability of positive ^{18}F-FSPG uptake in patients with active disease, as defined by the UCEIS or CDEIS. Specificity was defined as the probability of negative ^{18}F-FSPG uptake when the disease was not present. Bowel segment–level sensitivity and specificity were determined according to segmental UCEIS and CDEIS scores. Bowel segments that were not assessed by endoscopy were excluded from the analysis. The details are provided in the supplemental methods.

RESULTS

In Vivo Animal Studies

Twelve of 15 DSS-treated mice and 11 of 15 mice that underwent adoptive T-cell transfer met the eligibility criteria and completed the study. The control groups consisted of 6 and 10 mice, respectively. Clinical disease activity of DSS-treated mice on day 7 (median, 1.8; range, 0.7–3.3) and T-cell–transferred mice 8–12 wk after transfer (median, 2.5; range, 1.0–4.0) was significantly higher than that of their respective control groups ($P < 0.001$; Supplemental Fig. 1).

In DSS-treated mice, an increased ^{18}F-FSPG uptake in the colon was observed (Fig. 1). The SUV_{max} of ^{18}F-FSPG was significantly higher in the colons of DSS-treated than control mice (median, 2.1 [range, 0.5–3.9] vs. 0.7 [range, 0.5–1.9]; $P = 0.018$), as was the pathologic score derived from colon tissue (median, 14.2 [range,

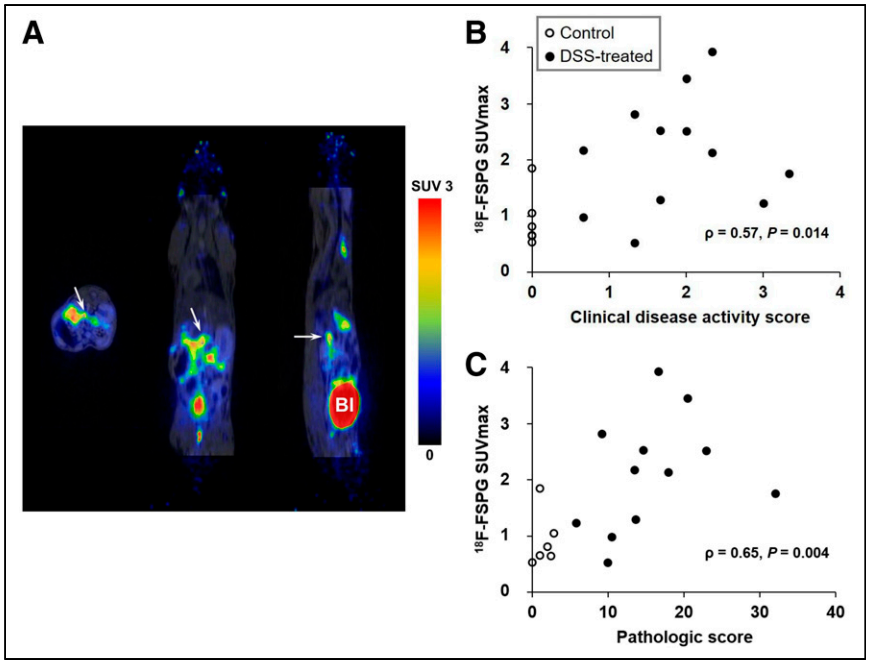

FIGURE 1. ^{18}F-FSPG imaging in DSS-treated mice. (A) Representative transaxial, coronal, and sagittal ^{18}F-FSPG PET/MR images of murine DSS-induced IBD model. Arrows indicate positive ^{18}F-FSPG uptake along colon. (B and C) Associations of colonic SUV_{max} with clinical disease activity (B) and pathologic score (C). Bl = bladder.

5.8–32.0] vs. 1.5 [range, 0–2.8]; $P < 0.001$). The SUV_{max} of ^{18}F-FSPG uptake was positively associated with clinical disease activity ($\rho = 0.57$, $P = 0.014$) and pathologic scores ($\rho = 0.65$, $P = 0.004$; Fig. 1; Supplemental Fig. 2).

Similarly, the SUV_{max} of colonic ^{18}F-FSPG uptake (median, 4.5 [range, 2.9–6.8] vs. 0.7 [range, 0.5–0.9]; $P < 0.001$) and the pathologic score derived from colon tissue (median, 8.3 [range, 6.4–14.8] vs. 0.8 [range, 0.4–1.6]; $P < 0.001$) were significantly higher in T-cell–transferred than in control mice (Fig. 2). The SUV_{max} of ^{18}F-FSPG uptake showed positive associations with clinical disease activity ($\rho = 0.74$, $P < 0.001$) and pathologic scores ($\rho = 0.74$, $P < 0.001$; Fig. 2; Supplemental Fig. 3).

Immunohistochemical staining of colon tissues revealed that xCT and GLUT1 were highly expressed in dendritic cells positive (+) for CD11c, in F4/80$^+$ macrophages, and in CD3$^+$ T cells in the lamina propria from mice with experimental colitis (Supplemental Fig. 4). In addition, immunohistochemical staining showed that xCT and GLUT1 were expressed in the epithelial cells of normal and inflamed mucosa.

Patients and ^{18}F-FSPG PET/CT Procedure

Between August 2018 and January 2019, 23 patients with IBD were assessed for initial eligibility and invited to participate in this prospective study. Three patients withdrew their consent before the injection of ^{18}F-FSPG. Finally, 10 patients with UC and 10 with CD were enrolled. All 20 patients completed ^{18}F-FSPG PET/CT as planned. The median administered activity per patient was 199.8 MBq (range, 192.4–214.6 MBq), and the median administered mass dose was 0.82 μg (range, 0.21–1.86 μg). Nineteen patients underwent colonoscopy, and 1 underwent sigmoidoscopy 1 d after ^{18}F-FSPG PET/CT. The demographic and baseline clinical characteristics are listed in Table 1. Six patients with UC (60%) and 8 with CD (80%) showed endoscopic evidence of active disease. Twelve (26%) of 47 bowel segments in patients with UC and 24 (59%) of 41 segments in patients with CD showed active inflammatory lesions.

^{18}F-FSPG Uptake in Patients

Readers determined that overall image quality was adequate for interpretation in all patients. The interreader agreements of visual assessment of ^{18}F-FSPG accumulation had κ-values of 0.70 (95% CI, 0.49–0.92) for patient-level analysis and 0.65 (95% CI, 0.57–0.73) for bowel segment–level analysis. Two readers disagreed on the presence of ^{18}F-FSPG accumulation in 2 (10%) of 20 patients and 10 (11%) of 95 bowels segments.

^{18}F-FSPG PET/CT was positive in 4 (67%) of the 6 UC patients with endoscopically active inflammation (Fig. 3) and correctly diagnosed endoscopic remission in 2 (50%) of the 4 patients (Supplemental Table 2). The 2 false-negative patients had scores of

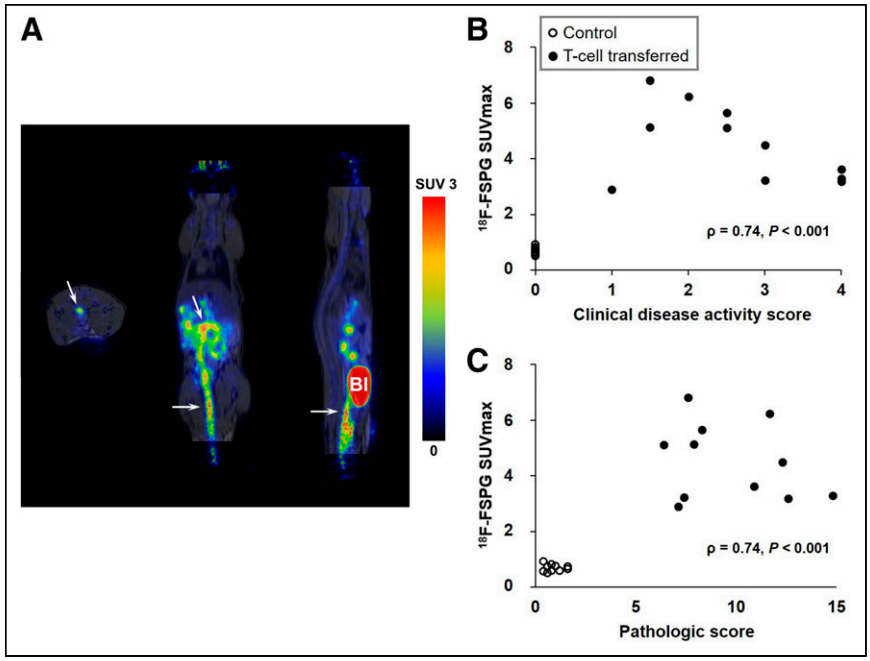

FIGURE 2. ^{18}F-FSPG imaging in T-cell–transferred mice. (A) Representative transaxial, coronal, and sagittal ^{18}F-FSPG PET/MR images of T-cell transfer–induced IBD model. Arrows indicate increased ^{18}F-FSPG uptake in colon. (B and C) Associations of colonic SUV_{max} with clinical disease activity (B) and pathologic score (C). Bl = bladder.

TABLE 1
Demographic and Clinical Characteristics

Characteristic	UC	CD
Asian (Korean)	10 (100%)	10 (100%)
Age (y)	42 (22–56)	28 (21–34)
Male	6 (60%)	9 (90%)
Body mass index (kg/m^2)	24.9 (17.1–36.9)	23.4 (18.7–30.0)
Smoking status		
Never	6 (60%)	6 (60%)
Former	3 (30%)	3 (30%)
Every day	1 (10%)	1 (10%)
Disease duration (mo)	40.2 (5.2–91.0)	55.8 (50.3–99.4)
Partial Mayo score	2 (0–4)	NA
Remission, 0–2	7 (70%)	
Mildly active, 3–5	3 (30%)	
CDAI	NA	91.89 (26.09–265.56)
Remission, <150		7 (70%)
Mildly active, 150–219		2 (20%)
Moderately active, 220–450		1 (10%)
Harvey–Bradshaw Index	NA	2 (1–12)
Remission, 0–4		8 (80%)
Mildly active, 5–7		1 (10%)
Moderately active, 8–16		1 (10%)
Hemoglobin (g/dL)	14.2 (10.5–15.2)	14.2 (9.4–17.5)
White blood cells ($\times 10^3/\mu L$)	7.7 (3.9–12.9)	6.9 (4.0–10.0)
Platelets ($\times 10^3/\mu L$)	310 (233–405)	287 (223–521)
Erythrocyte sedimentation (mm/h)	15 (3–53)	17 (2–105)
C-reactive protein (mg/dL)	0.11 (0.10–0.99)	0.43 (0.10–3.83)
Fecal calprotectin (μg/g)	65.1 (30.0–721)	116 (36.1–2,810)
UCEIS	2 (0–5)	NA
CDEIS	NA	9.8 (0.8–28.5)

NA = not applicable; CDAI = Crohn's Disease Activity Index.
Qualitative data are number and percentage; continuous data are median and range.

3 (Supplemental Fig. 5), and the 2 false-positives had scores of 4 (Supplemental Fig. 6). The sensitivity and specificity of ^{18}F-FSPG PET/CT in identifying active bowel segments were 75% (9/12) and 86% (30/35), respectively. All patients (n = 2) and bowel segments (n = 5) with superficial or deep ulcers were correctly identified.

All 8 CD patients with active inflammation (Fig. 4) and 2 with endoscopic remission were correctly diagnosed by ^{18}F-FSPG PET/CT (Supplemental Table 3). In a segment-based analysis, ^{18}F-FSPG PET/CT had a sensitivity of 71% (17/24) and a specificity of 94% (16/17), respectively. All 7 patients and 16 of 20 segments with superficial or deep ulcerations were correctly diagnosed.

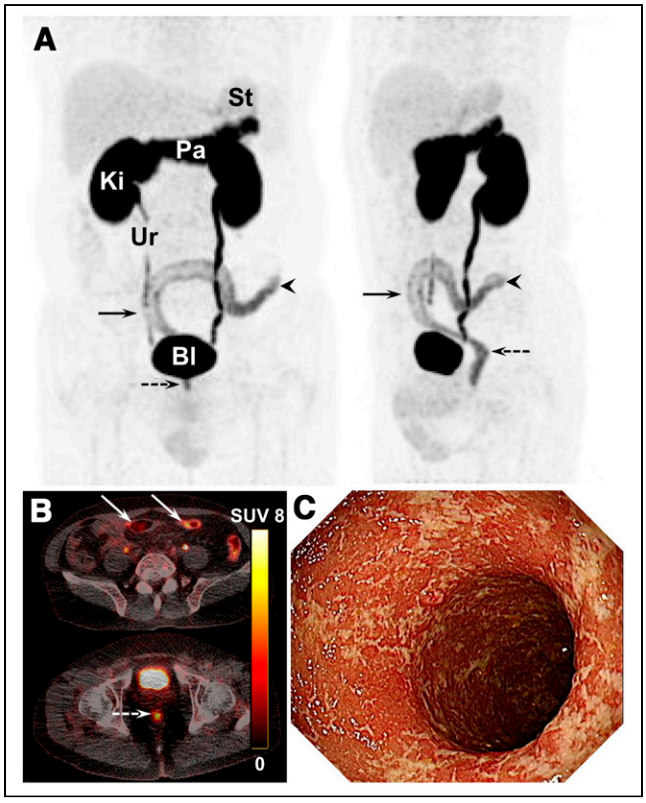

FIGURE 3. ^{18}F-FSPG PET/CT and endoscopic images of 55-y-old man with UC who presented with increased stool frequency, loose stools, hematochezia, and mild leukocytosis. His partial Mayo score was 4. (A and B) Maximum-intensity projection (A) and axial ^{18}F-FSPG (B) PET show increased ^{18}F-FSPG uptake along distal descending colon (arrowheads), sigmoid colon (arrows), and rectum (dashed arrows), with endoscopically active inflammation. (C) Endoscopic image of descending colon. Segmental UCEIS of ascending and transverse colon was 0, and that of descending colon, sigmoid colon, and rectum was 5. St = stomach; Pa = pancreas; Ki = kidneys; Ur = ureter; Bl = bladder.

Association Between ^{18}F-FSPG Uptake and Disease Activity

In patients with UC, the median SUV_{max} was 3.1 (range, 1.8–8.2). The summed SUV_{max} was strongly associated with the UCEIS (ρ = 0.79, P = 0.006) but not with the partial Mayo score, C-reactive protein, and fecal calprotectin (Supplemental Fig. 7). The segmental SUV_{max} (median, 2.2; range, 0.8–8.2) also showed strong associations with UCEIS (n = 47, ρ = 0.66; P < 0.001) and the Robarts Histopathology Index (n = 23, ρ = 0.64; P = 0.001).

The median SUV_{max} in patients with CD was 5.6 (range, 2.8–7.6). The summed SUV_{max} was strongly associated with the Crohn's Disease Activity Index (CDAI), C-reactive protein, fecal calprotectin, and the CDEIS (Supplemental Fig. 8). The segmental SUV_{max} (median, 2.9; range, 1.5–7.6) also showed a strong association with CDEIS (n = 41, ρ = 0.61; P < 0.001) but not with the Colonic and Ileal Global Histologic Disease Activity Score (n = 7, ρ = 0.33; P = 0.47).

Safety of ^{18}F-FSPG PET/CT

No adverse events were observed in patients with UC. However, 4 patients (40%) with CD had adverse events with mild

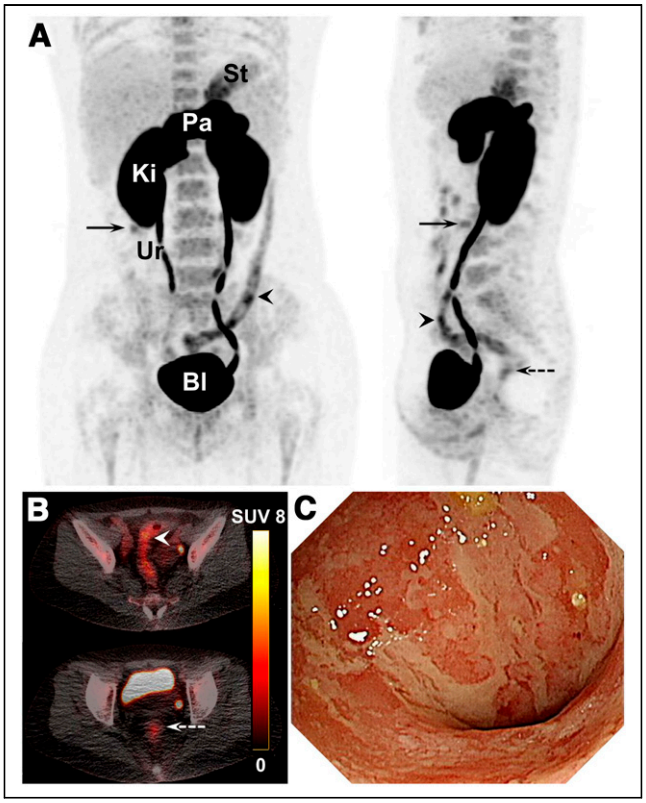

FIGURE 4. ^{18}F-FSPG PET/CT and endoscopic images of 26-y-old woman with CD who presented with abdominal pain and elevated C-reactive protein. Her CDAI was 102.47. (A and B) Maximum-intensity projection (A) and axial ^{18}F-FSPG (B) PET show increased ^{18}F-FSPG uptake in ileum (arrows), sigmoid and descending colon (arrowheads), and rectum (dashed arrows), which correlated well with endoscopic findings. Segmental CDEIS scores were 12 for ascending colon, 0 for transverse colon, 24 for descending and sigmoid colon, and 23 for rectum. Ileum was not assessed by colonoscopy. (C) Endoscopic image of rectum shows geographic and superficial ulcers, exudates, and streaks of coagulated blood. St = stomach; Pa = pancreas; Ki = kidneys; Ur = ureter; Bl = bladder.

intensity, including diarrhea, upper respiratory infection, arthritis, and dizziness. No adverse events were related to the study drug, and none of the patients experienced any serious adverse events or any clinically relevant changes in safety parameters.

Association Between xCT Expression and Disease Activity

Immunohistochemical staining showed that CD68$^+$, CD3$^+$, or CD66b$^+$ cells were present in the lamina propria of intestinal mucosa affected by UC (Supplemental Fig. 9) or CD (Supplemental Fig. 10). In addition, xCT was found to be expressed in the inflammatory and epithelial cells of all bowel segments. In patients with UC, the numbers of CD68$^+$xCT$^+$, CD3$^+$xCT$^+$, and CD66b$^+$xCT-negative cells in 22 bowel segments showed positive associations with UCEIS and SUV_{max} (Supplemental Table 4). By contrast, cytokeratin$^+$xCT$^+$ was negatively associated with UCEIS and SUV. In patients with CD, only the number of CD68$^+$xCT$^+$ cells in 7 bowel segments showed a significant association with CDEIS (Supplemental Table 5). Other cell populations showed no association with CDEIS or SUV.

DISCUSSION

Using mice with experimental IBD, we found that ^{18}F-FSPG accumulation in the colon was associated with disease activity indices and xCT expression in immune cells. Expansion of this study to patients, most of whom were clinically in remission or had mildly active IBD, showed that ^{18}F-FSPG PET/CT was accurate in diagnosing endoscopically active IBD and remission in patients and bowel segments. All patients with superficial or deep ulcers were correctly identified. Quantitative ^{18}F-FSPG uptake and xCT expression in immune cells were associated with endoscopic disease activity indices. ^{18}F-FSPG PET/CT was well tolerated, with no study drug–related adverse events. Our results suggest that ^{18}F-FSPG PET/CT can assess disease activity and distinguish between active IBD and mucosal healing, as determined endoscopically.

Although this study did not include participants across the entire range of disease activity, the subjects of this study may constitute a representative sample of those who would likely be the intended-use population for ^{18}F-FSPG PET/CT. All patients were evaluated by endoscopy after ^{18}F-FSPG PET/CT, with masked readers interpreting ^{18}F-FSPG PET/CT. Thus, there are no potential risks of bias or applicability regarding the accuracy of data. False-positives and false-negatives were likely due to an indeterminate zone for decision making. Greater experience with refined classification criteria may reduce the likelihood of patient misclassification. The positive association between quantitative ^{18}F-FSPG uptake and endoscopic assessment further supports the validity of ^{18}F-FSPG PET/CT. In patients with UC, the absence of a significant association between ^{18}F-FSPG uptake and conventional markers may be due to the inclusion of patients with mildly active disease and the small study sample.

We found that endoscopic assessment was positively associated with xCT expression by CD68$^+$ and CD3$^+$ immune cells in patients with UC and with xCT expression by CD68$^+$ cells in CD but not with xCT$^+$CD66b$^+$ cells. Although the small number of assessed bowel segments with CD may have precluded a consistent association, these results confirm the role of CD68$^+$xCT$^+$ macrophages in the antioxidative microenvironment of IBD (*10*). Our results also demonstrate that xCT expression is upregulated in human CD3$^+$ T cells, further strengthening the evidence for xCT expression and cystine uptake as regulators of T-cell function. These findings are consistent with results showing high initial rates of cystine and ^{18}F-FSPG uptake followed by decreases during a later phase of inflammation (*6,11,12*). xCT expression and cystine uptake in immune cells might mirror cellular concentrations of reactive oxygen species as well as metabolic activity (*20*). Taken together, these findings suggest that *in vivo* ^{18}F-FSPG PET/CT results may indicate broad changes in immune metabolism. Understanding of xCT in immune cells may also provide a pathologic tool to assess IBD activity.

Interestingly, the endoscopic assessment was negatively associated with xCT expression by cytokeratin$^+$ cells in patients with UC. xCT was expressed on the apical surfaces of the epithelial cells (Supplemental Figs. 9 and 10), where absorption occurs (*10,21*). This localization to absorptive sites suggests that system x_C^- plays a role in intestinal cystine transport (*21*) but does not involve ^{18}F-FSPG transport into the epithelial cells. The reason for the lack of association between GLUT1$^+$ immune cells and endoscopic assessment is not apparent but may be related to the persistent glucose hypermetabolism in healing tissue after inflammation (*22,23*).

Radiation exposure is an important limitation in using ^{18}F-FSPG PET/CT to assess disease activity, mainly because most of these patients are relatively young. Current guidelines recommend using cross-sectional imaging modalities that do not entail exposure to ionizing radiation when it is likely that serial examinations are required (*1*). A per-patient dose of 200 MBq of ^{18}F-FSPG would result in a mean effective dose of 4.0 ± 0.2 mSv, including the dose from CT (*24*). These doses can be significantly reduced using

highly sensitive PET/CT systems (*25*). Study protocols that allow a low dose of ^{18}F-FSPG can reduce the radiation dose by as much as 75% without clinical detriment (*26*).

This study had several limitations. First, the diagnostic validity should be interpreted with caution because of the small number of included patients and the exploratory nature of the study. Additional studies on larger numbers of patients are required to validate our initial results. Second, the assessment of IBD activity was based on endoscopic findings. Thus, comparisons between endoscopy and ^{18}F-FSPG PET/CT may be limited because the actual sites of endoscopic evaluation may not precisely match those of ^{18}F-FSPG uptake, thereby underestimating the accuracy of ^{18}F-FSPG PET/CT for evaluating bowel segments.

CONCLUSION

^{18}F-FSPG PET/CT imaging of system x_C^- in immune cells can noninvasively assess IBD activity and remission of the entire bowel without the need for bowel preparation and safety issues related to invasive endoscopic procedures. Assessment of system x_C^- expression by immune cells may provide diagnostic information on the dysregulated immune responses responsible for chronic active inflammation.

DISCLOSURE

This research was sponsored by the Asan Foundation (Seoul, Republic of Korea) and financially supported by National Research Foundation grants NRF-2016M2A2A7A03913219 and NRF-2019R1A2C209022213 funded by the Korea Ministry of Science and ICT, Republic of Korea, and by the Korea Health Technology R&D Project through the Korea Health Industry Development Institute, funded by the Ministry of Health and Welfare, Republic of Korea (grant HI18C2383). The funders had no role in the conceptualization or design of the study; in the collection, analysis, and interpretation of the data; in the writing of the manuscript; or in the decision to submit the manuscript for publication. Norman Koglin and Andrew Stephens report personal fees from Life Molecular Imaging GmbH (employment) during the conduct of the study and are listed as coinventors on a patent application entitled "[F-18]-labeled L-glutamic acid and L-glutamine derivatives (I), their use and processes for their preparation; US 9,308,282", which is owned by Life Molecular Imaging. Dae Hyuk Moon reports receiving grants from the National Research Foundation of Korea, the Korea Health Industry Development Institute, and Life Molecular Imaging GmbH. No other potential conflict of interest relevant to this article was reported.

KEY POINTS

QUESTION: Does *in vivo* assessment of system x_C^- in immune cells provide information on the dysregulated immune responses responsible for chronic active inflammation in IBD, thereby assessing the disease activity?

PERTINENT FINDINGS: System x_C^- expression in immune cells was associated with endoscopic disease activity indices. PET imaging of system x_C^- was accurate in diagnosing endoscopically active disease and remission in patients and bowel segments.

IMPLICATIONS FOR PATIENT CARE: PET imaging of system x_C^- may noninvasively assess disease activity and remission without the need for bowel preparation or the safety issues related to endoscopic procedures.

REFERENCES

1. Lichtenstein GR, Loftus EV, Isaacs KL, Regueiro MD, Gerson LB, Sands BE. ACG clinical guideline: management of Crohn's disease in adults. *Am J Gastroenterol.* 2018;113:481–517.
2. Rubin DT, Ananthakrishnan AN, Siegel CA, Sauer BG, Long MD. ACG clinical guideline: ulcerative colitis in adults. *Am J Gastroenterol.* 2019;114:384–413.
3. de Souza HS, Fiocchi C. Immunopathogenesis of IBD: current state of the art. *Nat Rev Gastroenterol Hepatol.* 2016;13:13–27.
4. Dearling JL, Daka A, Veiga N, Peer D, Packard AB. Colitis immunoPET: defining target cell populations and optimizing pharmacokinetics. *Inflamm Bowel Dis.* 2016;22:529–538.
5. Lewerenz J, Hewett SJ, Huang Y, et al. The cystine/glutamate antiporter system x_C^- in health and disease: from molecular mechanisms to novel therapeutic opportunities. *Antioxid Redox Signal.* 2013;18:522–555.
6. Sato H, Fujiwara K, Sagara J, Bannai S. Induction of cystine transport activity in mouse peritoneal macrophages by bacterial lipopolysaccharide. *Biochem J.* 1995; 310:547–551.
7. Nabeyama A, Kurita A, Asano K, et al. xCT deficiency accelerates chemically induced tumorigenesis. *Proc Natl Acad Sci USA.* 2010;107:6436–6441.
8. Garg SK, Yan Z, Vitvitsky V, Banerjee R. Differential dependence on cysteine from transsulfuration versus transport during T cell activation. *Antioxid Redox Signal.* 2011;15:39–47.
9. Levring TB, Hansen AK, Nielsen BL, et al. Activated human CD4+ T cells express transporters for both cysteine and cystine. *Sci Rep.* 2012;2:266.
10. Sido B, Lasitschka F, Giese T, et al. A prominent role for mucosal cystine/cysteine metabolism in intestinal immunoregulation. *Gastroenterology.* 2008;134:179–191.
11. Koglin N, Mueller A, Berndt M, et al. Specific PET imaging of x_C^- transporter activity using a ^{18}F-labeled glutamate derivative reveals a dominant pathway in tumor metabolism. *Clin Cancer Res.* 2011;17:6000–6011.
12. Chae SY, Choi CM, Shim TS, et al. Exploratory clinical investigation of (4*S*)-4-(3-^{18}F-fluoropropyl)-L-glutamate PET of inflammatory and infectious lesions. *J Nucl Med.* 2016;57:67–69.
13. Baek S, Mueller A, Lim YS, et al. (4*S*)-4-(3-^{18}F-fluoropropyl)-L-glutamate for imaging of x_C^- transporter activity in hepatocellular carcinoma using PET: preclinical and exploratory clinical studies. *J Nucl Med.* 2013;54:117–123.
14. Li Y, Beiderwellen K, Nensa F, et al. [^{18}F]FDG PET/MR enterography for the assessment of inflammatory activity in Crohn's disease: comparison of different MRI and PET parameters. *Eur J Nucl Med Mol Imaging.* 2018;45:1382–1393.
15. Tenhami M, Virtanen J, Kauhanen S, et al. The value of combined positron emission tomography/magnetic resonance imaging to diagnose inflammatory bowel disease: a prospective study. *Acta Radiol.* 2021;62:851–857.
16. Shih IL, Wei SC, Yen RF, et al. PET/MRI for evaluating subclinical inflammation of ulcerative colitis. *J Magn Reson Imaging.* 2018;47:737–745.
17. Li Y, Khamou M, Schaarschmidt BM, et al. Comparison of ^{18}F-FDG PET-MR and fecal biomarkers in the assessment of disease activity in patients with ulcerative colitis. *Br J Radiol.* 2020;93:20200167.
18. Walsh AJ, Bryant RV, Travis SP. Current best practice for disease activity assessment in IBD. *Nat Rev Gastroenterol Hepatol.* 2016;13:567–579.
19. Ahn J, Jin M, Song E, et al. Immune profiling of advanced thyroid cancers using fluorescent multiplex immunohistochemistry. *Thyroid.* 2021;31:61–67.
20. Siska PJ, Kim B, Ji X, et al. Fluorescence-based measurement of cystine uptake through xCT shows requirement for ROS detoxification in activated lymphocytes. *J Immunol Methods.* 2016;438:51–58.
21. Burdo J, Dargusch R, Schubert D. Distribution of the cystine/glutamate antiporter system x_C^- in the brain, kidney, and duodenum. *J Histochem Cytochem.* 2006;54: 549–557.
22. Lazzeri E, Bozzao A, Cataldo MA, et al. Joint EANM/ESNR and ESCMID-endorsed consensus document for the diagnosis of spine infection (spondylodiscitis) in adults. *Eur J Nucl Med Mol Imaging.* 2019;46:2464–2487.
23. Priftakis D, Riaz S, Zumla A, Bomanji J. Towards more accurate ^{18}F-fluorodeoxyglucose positron emission tomography (^{18}F-FDG PET) imaging in active and latent tuberculosis. *Int J Infect Dis.* 2020;92(suppl):S85–S90.
24. Smolarz K, Krause BJ, Graner FP, et al. (*S*)-4-(3-^{18}F-fluoropropyl)-L-glutamic acid: an ^{18}F-labeled tumor-specific probe for PET/CT imaging: dosimetry. *J Nucl Med.* 2013;54:861–866.
25. Surti S, Viswanath V, Daube-Witherspoon ME, Conti M, Casey ME, Karp JS. Benefit of improved performance with state-of-the art digital PET/CT for lesion detection in oncology. *J Nucl Med.* 2020;61:1684–1690.
26. Alberts I, Sachpekidis C, Prenosil G, et al. Digital PET/CT allows for shorter acquisition protocols or reduced radiopharmaceutical dose in [^{18}F]-FDG PET/CT. *Ann Nucl Med.* 2021;35:485–492.